Asymmetric Low-Voltage Ride-Through Scheme and Dynamic Voltage Regulation in Distributed Generation Units

Masoud M. Shabestary
Electrical and Computer Engineering
University of Alberta
Edmonton, Canada
masoud2@ualberta.ca

Shahed Mortazavian
Electrical and Computer Engineering
University of Alberta
Edmonton, Canada
shahed1@ualberta.ca

Yasser A-R. I. Mohamed
Electrical and Computer Engineering
University of Alberta
Edmonton, Canada
yasser2@ualberta.ca

***Abstract* — Most grid codes mainly focus on the low-voltage ride-through (LVRT) requirements under balanced grid faults, and simply provide the LVRT curves which only apply for the positive-sequence voltage value. Under short-term asymmetric faults, this brings some shortcomings: i) disconnecting the large units under temporary unbalanced faults worsens the situation most of the time, and may cause cascaded outages; ii) a reconnection process is required after the fault is cleared; iii) it is not an economical option, and the power may be wasted. Therefore, a new regulation scheme, called asymmetric low-voltage ride-through (ALVRT), is proposed in this paper. The ALVRT scheme is intended to provide the allowable margins for each phase voltage magnitude rather than for just positive-sequence voltage. This aids the large converter-interfaced distributed generation units not only ride through the asymmetrical grid faults, but also support the grid with a seamless transition over the fault and enhance the power system reliability. A new voltage regulation method is also proposed to address the ALVRT specifications. The successful results of the proposed regulation scheme and voltage support method are verified using simulation test cases.**

***Index Terms* — Fault ride through, grid codes, grid-connected converters, positive and negative sequence control, unbalanced faults, voltage regulation.**

I. Introduction

Increasing growth is expected for exploiting renewable and green energy resources in coming years. This will shift the electrical network paradigm toward increasing integration of distributed generation (DG) units [1], [2]. Grid-connected converters (GCCs) have been identified to be critical components for DGs thriving integration. Robust and reliable operation of high power GCCs, under various abnormalities, has thus become a substantial challenge for system operator and reinforced existing concerns regarding their influences on the grid stability [3]-[7]. The combination of growing DG sources with large applications of modern loads causes more vulnerability to voltage sags, swells, and unbalanced conditions [8]. In this sense, the distant grid faults can significantly harm the operation of GCCs. However, GCCs can be smartly controlled for riding through the short-term faults and delivering ancillary services to improve the grid stability and reliability [9].

Recent grid codes from different countries [10]-[16] render certain voltage magnitude curves above which the GCC should withstand the short-term symmetrical faults. This is well known as low-voltage ride-through (LVRT) requirements. In order to address the stability concerns, the performance of DG systems must be improved to meet the LVRT requirements in each country. Numerous efforts have thus been carried out to fulfill these requirements and improve the LVRT capabilities of distributed generation units [17]-[29].

Some countries (such as Germany, England and Ireland [13]-[15]) mandate reactive current injection (RCI) requirements by wind power plants during the grid faults. The RCI aims to support and rapidly restore the system voltage, in much the same way as a conventional synchronous generators increases its excitation during faults via automatic voltage regulator action [11]. German grid code, E.ON [13], forces wind farms to support grid voltage with additional reactive current during a voltage dip, amounting to at least 2% of the rated current for each percent of the voltage dip. The characteristic refers to the voltage at the grid connection point, and only applies when the fault is a symmetrical voltage dip. The grid codes in Britain [14] and Ireland [15] denote that wind power plants must deliver their maximum reactive current during a symmetrical voltage dip. Also, the wind power plants are required to be able to inject reactive power within 150 ms (7.5 cycles) of grid recovery, according to the Spanish grid code [16]. However, most of the codes, to date, have not considered specific RCI requirements in the case of unbalanced network fault, whereas its probability in transmission systems are much higher compared to the balanced fault. Thus, filling this gap, in grid code updated versions, is very crucial for the increasing integration of DG units. Hereupon, the main contribution of this paper is suggesting the new requirements in the case of short-term asymmetrical voltage sags, named as asymmetric low-voltage ride-though (ALVRT) scheme.

Second, the dynamic voltage regulation (DVR) method is proposed. The idea is to *i*) regulate the three-phase voltages above the ALVRT curves and within dynamic

margins, *ii*) reduce the voltage unbalance factor down to a desired range, and *iii*) be adaptive to the LVRT codes in different countries. Applying the proposed technique under unbalanced conditions, all the three-phase voltages will be time-varyingly regulated within two dynamic thresholds above the ALVRT curves. Therefore, the proposed method is dynamically adaptive to different codes. The effectiveness of the proposed analytical expressions are validated by selected simulation test cases in Section VII. Finally, Section VIII concludes the work.

II. Proposed Asymmetrical Low-Voltage Ride-Through (ALVRT) Scheme

As stated earlier, recent grid codes provide the well-known LVRT curves of Fig 1 above which the generating plant must not disconnect from the grid. These curves are only applicable under balanced voltage sags or only on the positive-sequence value of the voltage. However, Fig 2 demonstrates the proposed curves in this paper. These curves are applicable under any fault condition (balanced or unbalanced) since they are applied on the phase voltage magnitudes. These are named as the ALVRT curves in this paper. According to Fig 2, if each phase voltage magnitude can be regulated inside the highlighted green area, the generating plant can stay connected to the grid. During the successful ALVRT period, the phase current limits must be respected. In this period, the reactive current injection has the priority leading to the active power curtailment due to the phase current limitation. During an unbalanced short term fault, the following two conditions should be respected:

1) all three phase voltages are (or can be regulated) in the highlighted green area
2) the phase currents do not exceed the maximum phase current limit,

If the above conditions can be achieved by a proper voltage support strategy, the GCC experiences a successful ride-through under the short-term unbalanced fault.

In this paper, two sets of curves are derived as the allowed boundaries for the voltage magnitudes in each phase. It is intended to regulate the phase voltage magnitudes within these curves. The first curve is adapted from the German Grid Code [13] and indicated in Fig 2(b). This curve is named German-ALVRT in this paper. Furthermore, another set of curves is presented in Fig 2(c) which has been adapted from IEEE-1547 standard [19].

III. Proposed Dynamic Voltage Regulation (DVR) Strategy

A distant grid fault or unbalanced loading can cause unbalanced voltage at the point of common coupling (PCC).

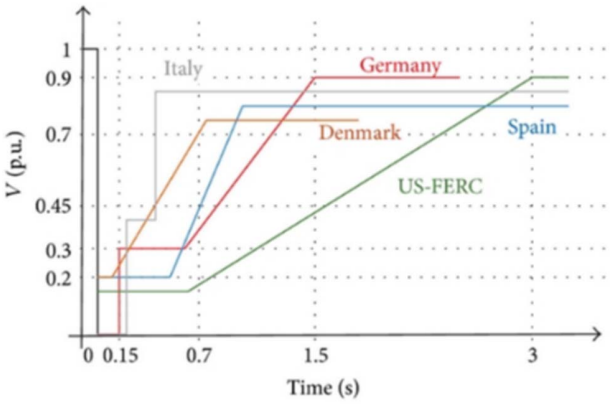

Fig 1. LVRT curves of different grid codes [18]

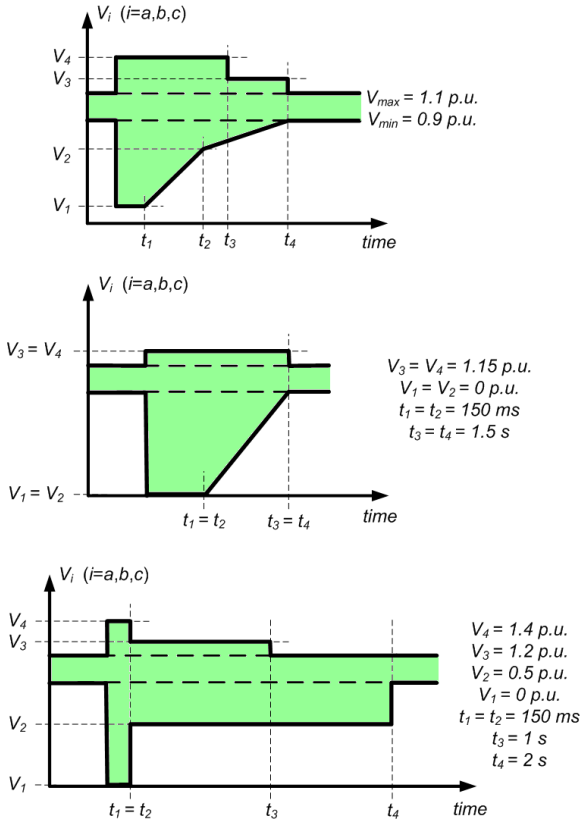

Fig 2. Proposed ALVRT curves: (a) a generic scheme, (b) German grid code adapted ALVRT curve, (c) IEEE-1547 adapted ALVRT curve.

The voltage vector can be represented in the positive and negative sequences, for any unbalanced condition:

$$v^{+}=\begin{bmatrix}v_{\alpha}^{+}\\ v_{\beta}^{+}\end{bmatrix}=\begin{bmatrix}V^{+}\cos(\omega t+\delta^{+})\\ V^{+}\sin(\omega t+\delta^{+})\end{bmatrix}\qquad v^{-}=\begin{bmatrix}v_{\alpha}^{-}\\ v_{\beta}^{-}\end{bmatrix}=\begin{bmatrix}V^{-}\cos(\omega t+\delta^{-})\\ -V^{-}\sin(\omega t+\delta^{-})\end{bmatrix} \quad (1)$$

where δ^{+} and δ^{-} are, respectively, the phase angles of the positive and negative voltage sequences. In order to achieve a flexible supportive performance, the injected current by a GCC is determined via four components (i.e. positive/negative and active/reactive components) as

$$i = i_p^{+} + i_p^{-} + i_q^{+} + i_q^{-} \quad (2)$$

where the vectors with superscripts "+"/"-" and subscripts "p"/"q" denote the positive/negative and active/reactive components, respectively. The reactive current can be also written in the $\alpha\beta$ reference frame as

$$\begin{bmatrix} i_{q,\alpha} \\ i_{q,\beta} \end{bmatrix} = \begin{bmatrix} I_{q+}\sin(\omega t+\delta^{+}) - I_{q-}\sin(\omega t+\delta^{-}) \\ -I_{q+}\cos(\omega t+\delta^{+}) - I_{q-}\cos(\omega t+\delta^{-}) \end{bmatrix} \tag{3}$$

To regulate the phase voltage magnitudes by positive and negative current control, their values should be obtained from the positive-, negative-, and zero-sequence values of the voltage by

$$\begin{aligned} V_a &= \sqrt{\left(V^{+}\right)^2+\left(V^{-}\right)^2+2\left(V^{+}\right)\left(V^{-}\right)\cos(\gamma)}+\left(V^{0}\right)\cos\left(\phi^{0}\right) \\ V_b &= \sqrt{\left(V^{+}\right)^2+\left(V^{-}\right)^2+2\left(V^{+}\right)\left(V^{-}\right)\cos\left(\gamma-\tfrac{2\pi}{3}\right)}+\left(V^{0}\right)\cos\left(\phi^{0}+\tfrac{2\pi}{3}\right) \\ V_c &= \sqrt{\left(V^{+}\right)^2+\left(V^{-}\right)^2+2\left(V^{+}\right)\left(V^{-}\right)\cos\left(\gamma+\tfrac{2\pi}{3}\right)}+\left(V^{0}\right)\cos\left(\phi^{0}-\tfrac{2\pi}{3}\right) \end{aligned} \tag{4}$$

Then, the reference values for the positive and negative voltage values should be obtained from the reference values for the maximum and minimum phase voltage magnitudes V_{max} and V_{min}:

$$\begin{aligned} \left(V_{ref}^{+}\right)^2 &= \frac{xV_y^2-yV_x^2+\sqrt{\left(xV_y^2-yV_x^2\right)^2-\left(V_y^2-V_x^2\right)^2}}{2(x-y)} \\ \left(V_{ref}^{-}\right)^2 &= \frac{xV_y^2-yV_x^2-\sqrt{\left(xV_y^2-yV_x^2\right)^2-\left(V_y^2-V_x^2\right)^2}}{2(x-y)} \end{aligned} \tag{5}$$

where,

$$\begin{aligned} V_y &= V_{\min}-V^{0}y_0, \\ V_x &= \min\left(V_{\max},V_{\min}+\max\{V_a,V_b,V_c\}-\min\{V_a,V_b,V_c\}\right)-V^{0}x_0 \\ y_0 &= \min\left(\cos\left(\phi^{0}\right),\cos\left(\phi^{0}-\tfrac{2\pi}{3}\right),\cos\left(\phi^{0}+\tfrac{2\pi}{3}\right)\right), \\ x_0 &= \max\left(\cos\left(\phi^{0}\right),\cos\left(\phi^{0}-\tfrac{2\pi}{3}\right),\cos\left(\phi^{0}+\tfrac{2\pi}{3}\right)\right) \end{aligned} \tag{6}$$

The reference values for reactive currents in (3) can be obtained by the values calculated for V_{ref}^{+} and V_{ref}^{-} form (5):

$$I_{q+}^{ref}=\frac{V_{ref}^{+}-V_g^{+}}{X_g}, \qquad I_{q-}^{ref}=\frac{V_g^{-}-V_{ref}^{-}}{X_g} \tag{7}$$

Instead of using the constant V_{max} and V_{min} values in (6), it is proposed in this paper to dynamically obtain their values according to the applied ALVRT curve. Fig 3 simply shows that the average of the V_{max} and V_{min} boundaries in the ALVRT scheme is obtained. Then, a constant quantity (e.g. ±0.1p.u.) is added to the average value. In order to have a smooth transient behaviour, the result passes through the low-pass filters. Finally, the reference maximum and minimum phase voltage magnitudes V_{max} and V_{min} are obtained. Fig 4 shows the obtained reference values for the maximum and minimum phase voltage magnitudes for two proposed ALVRT curves in the previous section. It illustrates the obtained V_{max} and V_{min} values for both German-ALVRT and IEEE-ALVRT curves using the procedure indicated in Fig 3. If the dashed pink lines of Fig 4 are used in (6), the phase voltages will be regulated within the proposed ALVRT boundaries.

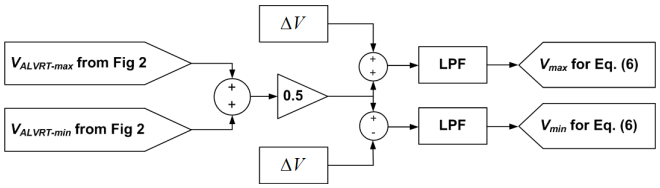

Fig 3. Procedure to determine the V_{max} and V_{min} values.

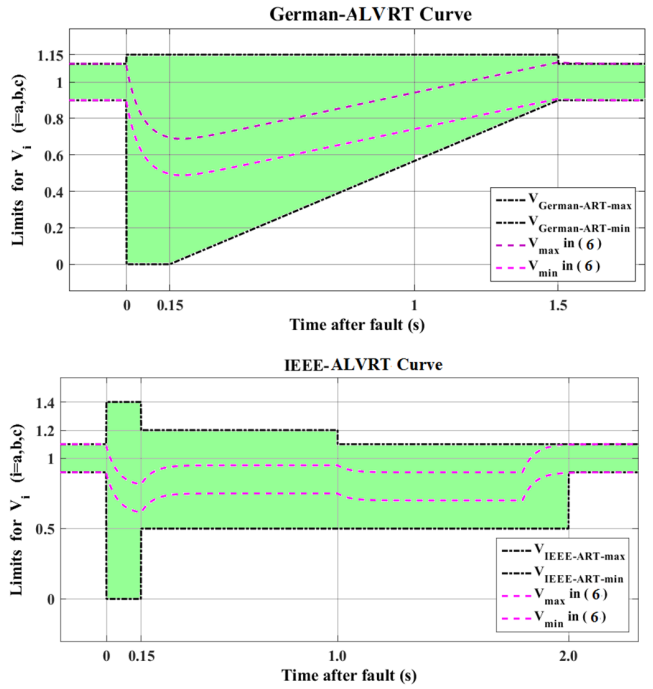

Fig 4. Determined V_{max} and V_{min} values for both German-ALVRT and IEEE-ALVRT curves using the procedure indicated in Fig 3.

IV. Simulation Results

To show the effectiveness of the ALVRT scheme, four test cases have been implemented in this section. The results of the proposed voltage regulation method are also compared to three conventional strategies, i.e. mixed sequence injection (MSI) [26], positive and negative-sequence based voltage regulation (PNVR) [27], and grid code required voltage support (GCRVS) [13] strategies. Four test cases examined in this section are as follows:

1) Test-Case A: solid one-phase fault (1.0 p.u. voltage dip on phase A) from t=0.2s to t=1.2s and applying German-ALVRT scheme.
2) Test-Case B: two-phase fault (0.7 p.u. voltage dips on phases A and B) from t=0.2s to t=1.2s and applying German-ALVRT scheme.

3) Test-Case C: solid one-phase fault (1.0 p.u. voltage dip on phase A) from t=0.2s to t=1.2s and applying IEEE-ALVRT scheme.
4) Test-Case D: solid two-phase fault (1.0 p.u. voltage dips on phases A and B) from t=0.2s to t=1.2s and applying IEEE-ALVRT scheme.

In all of these test cases, phase current limit is taken 1 p.u. Three traditional strategies are selected here to be compared with the proposed DVR strategy (i.e. MSI in Test-Case A and D, GCRVS in Test-Case B, and PNVR in Test-Case C). Fig 5 shows the results of applying the MSI strategy in Test-Case A where the ALVRT scheme fails. It is because the voltage magnitude of phase A exits the allowed ALVRT boundary at t=0.94s. However, the proposed DVR strategy illustrates a successful ride-through as presented in Fig 6.

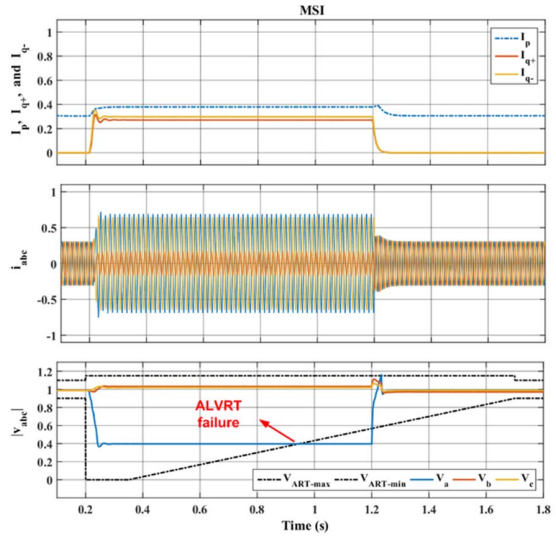

Fig 5. Test-Case A: results of conventional MSI strategy [26], (a) active/reactive currents commands, (b) phase currents, and (c) magnitudes of phase voltages.

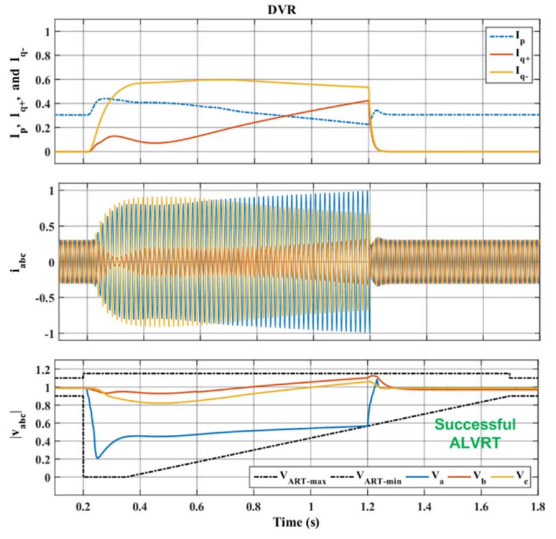

Fig 6. Test-Case A: results of the proposed DVR strategy, (a) active/reactive currents commands, (b) phase currents, and (c) magnitudes of phase voltages.

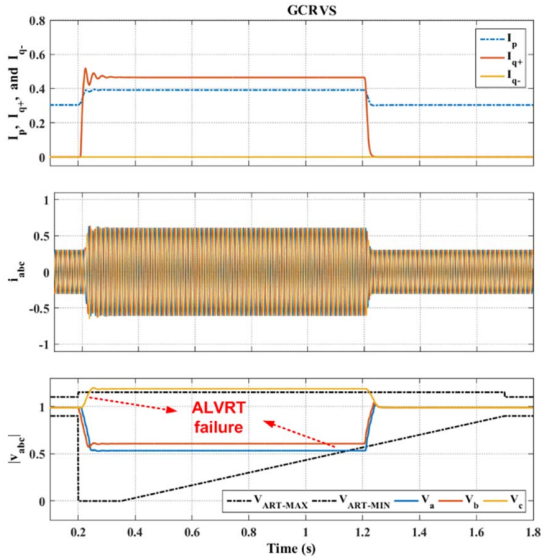

Fig 7. Test-Case B: results of the conventional GCR strategy [13], (a) active/reactive currents commands, (b) phase currents, and (c) magnitudes of phase voltages.

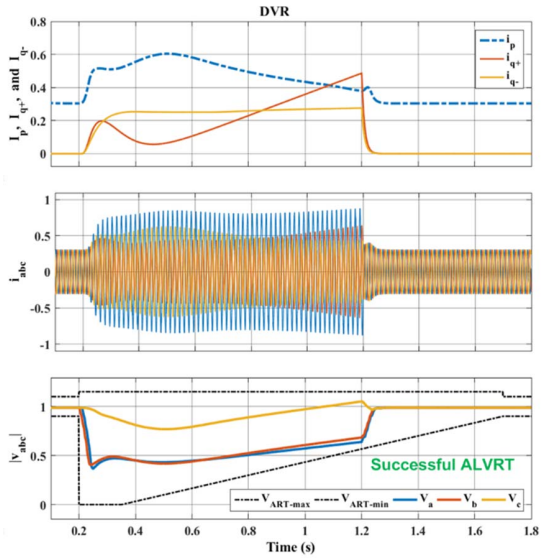

Fig 8. Test-Case B: results of the proposed DVR strategy, (a) active/reactive currents commands, (b) phase currents, and (c) magnitudes of phase voltages.

TABLE I. Test System Parameters

Z_g (Ω)	j0.2	V_{DC} (V)	2000
Z (mΩ)	1	$V_{L\text{-}L\ RMS}$ (V)	690
Z_f (mΩ)	0.8	f (Hz)	60
I_{rate} (A)	840	S (MVA)	1

Based on the obtained positive/negative and reactive/active current commands of Fig 6(a), both conditions of the German-ALVRT scheme are completely satisfied, i.e. phase currents do not exceed the phase current limit (Fig 6(b)) and phase voltage magnitudes remain inside the German-ALVRT boundaries (Fig 6(c)). Fig 7 shows the results of the traditional GCRVS strategy in Test-Case B. According to these results, the GCRVS fails to have a successful ride-through since the voltage magnitude of phases C and A exits the proposed German-ALVRT

boundaries. In contrary, Fig 8 demonstrates the successful results of the proposed strategy in this test case where the obtained current commands (Fig 8(a)) lead to phase voltage regulation inside the German-ALVRT boundaries (Fig 8(c)) and respecting phase current limitation (Fig 8(b)). Also, Test-Case C is examined to compare the conventional PNVR strategy and the DVR strategy. Fig 9 presents the results of the PNVR strategy in Test-Case B where the IEEE-ALVRT is failed due to the over-voltage of phase C. However, the DVR illustrates successful results as indicated in Fig 10.

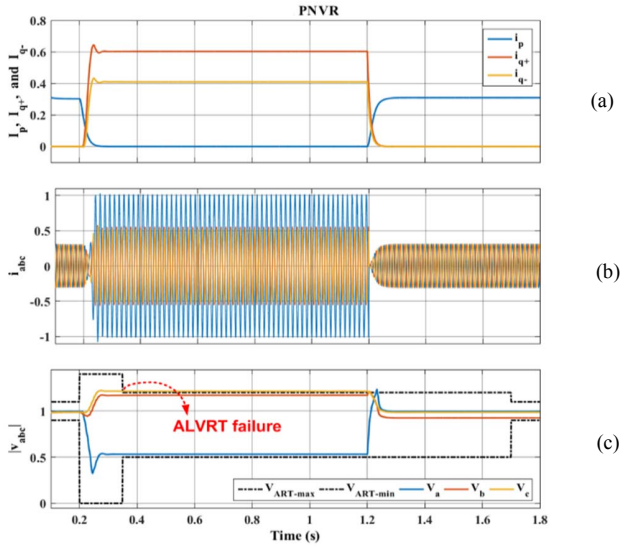

Fig 9. Test-Case C: results of the conventional PNVR strategy [27], (a) active/reactive currents commands, (b) phase currents, and (c) magnitudes of phase voltages.

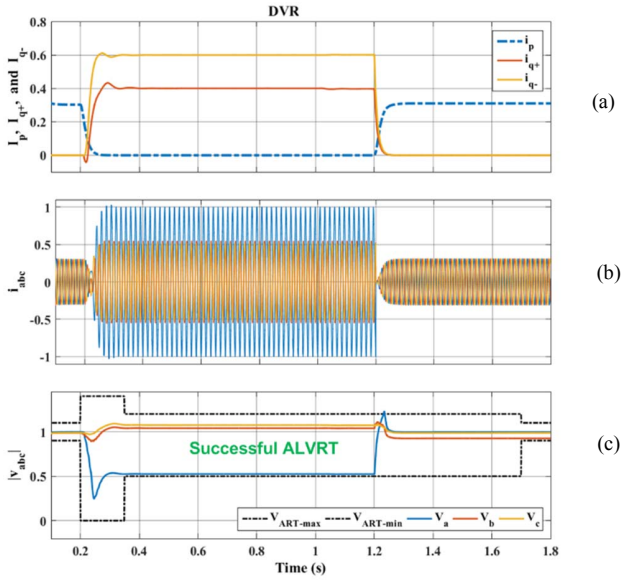

Fig 10. Test-Case C: results of the proposed DVR strategy, (a) active/reactive currents commands, (b) phase currents, and (c) magnitudes of phase voltages.

For further evaluation, a very severe two-phase-to-ground voltage dip (i.e. voltage magnitude of phases A and B becomes zero for 1s) is studied in Test-Case D. Fig 11 shows that the conventional MSI strategy is unable to have a successful ride through due to under-voltage in phase B after 150 ms of the fault occurrence (Fig 11(c)). On the other side, the proposed DVR demonstrates the successful ride-through based on IEEE-ALVRT as shown in Fig 12. Even under this severe test case, the DVR strategy is able to regulate the phase voltage magnitudes inside the proposed IEEE-ALVRT boundaries and simultaneously respect the phase current limitation.

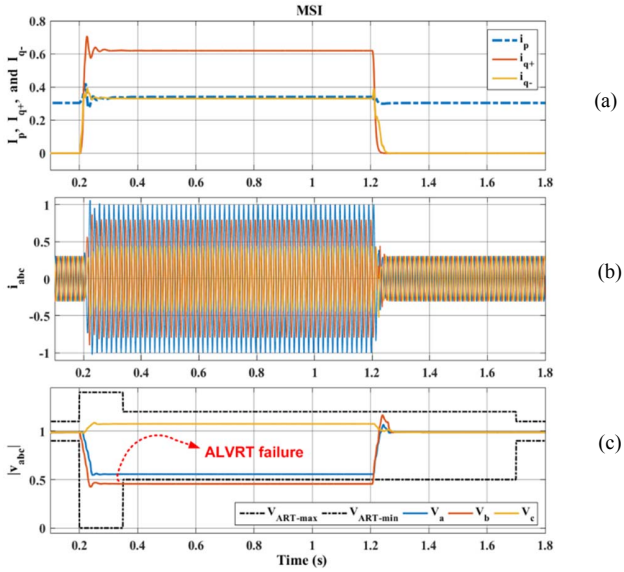

Fig 11. Test-Case D: results of the conventional MSI strategy [26], (a) active/reactive currents commands, (b) phase currents, and (c) magnitudes of phase voltages.

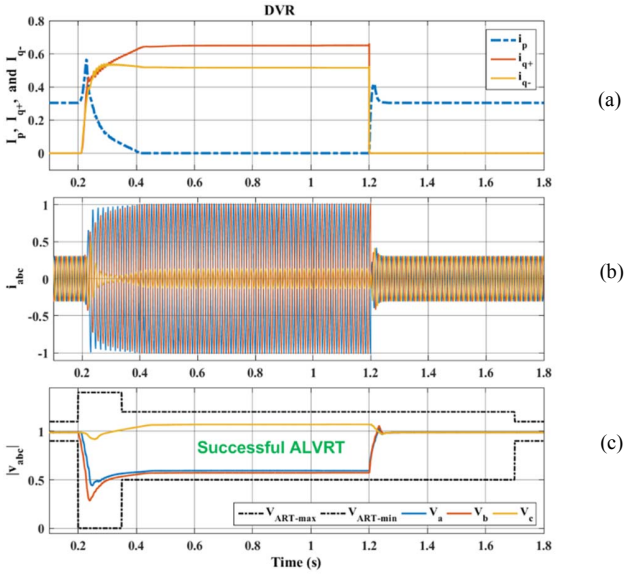

Fig 12. Test-Case D: results of the proposed DVR strategy, (a) active/reactive currents commands, (b) phase currents, and (c) magnitudes of phase voltages.

V. CONCLUSION

This paper put forth the necessity of the asymmetric low-voltage ride-through (ALVRT) regulation scheme. The ALVRT scheme prescribes proper specifications on the regulation of the phase voltage magnitudes by appropriate positive and negative reactive currents injection and simultaneously respecting the phase current limitation. An advanced dynamic voltage regulation method was also proposed to address the ALVRT specifications. The proposed method supports the connection voltage under any unbalanced faults. The proposed method aims to regulate all three phase voltages inside the ALVRT boundaries within the dynamic margins which are adaptive to the codes of different countries. The performance of the proposed scheme and method were successfully verified by simulation results.

REFERENCES

[1] Z. Chen, J. M. Guerrero, and F. Blaabjerg, "A review of the state of the art of power electronics for wind turbines," *IEEE Trans. Power Electron.*, vol. 24, no. 8, pp. 1859–1875, Aug. 2009.

[2] W. Sinsukthavorn, E. Ortjohann, A. Mohd, N. Hamsic, and D. Morton, "Control strategy for three-/four-wire-inverter-based distributed generation," *IEEE Trans. Ind. Electron.*, vol. 59, no. 10, pp. 3890–3899, Oct. 2012.

[3] A. Moawwad, M. S. El Moursi and W. Xiao, "Advanced Fault Ride-Through Management Scheme for VSC-HVDC Connecting Offshore Wind Farms," in *IEEE Transactions on Power Systems*, vol. 31, no. 6, pp. 4923-4934, Nov. 2016.

[4] M. I. Daoud, A. M. Massoud, A. S. Abdel-Khalik, A. Elserougi and S. Ahmed, "A Flywheel Energy Storage System for Fault Ride Through Support of Grid-Connected VSC HVDC-Based Offshore Wind Farms," in *IEEE Transactions on Power Systems*, vol. 31, no. 3, pp. 1671-1680, May 2016.

[5] D. Shin, K. J. Lee, J. P. Lee, D. W. Yoo and H. J. Kim, "Implementation of Fault Ride-Through Techniques of Grid-Connected Inverter for Distributed Energy Resources With Adaptive Low-Pass Notch PLL," in *IEEE Transactions on Power Electronics*, vol. 30, no. 5, pp. 2859-2871, May 2015.

[6] H. M. Hasanien, "An Adaptive Control Strategy for Low Voltage Ride Through Capability Enhancement of Grid-Connected Photovoltaic Power Plants," in *IEEE Transactions on Power Systems*, vol. 31, no. 4, pp. 3230-3237, July 2016.

[7] S. I. Nanou and S. A. Papathanassiou, "Grid Code Compatibility of VSC-HVDC Connected Offshore Wind Turbines Employing Power Synchronization Control," in *IEEE Transactions on Power Systems*, vol. 31, no. 6, pp. 5042-5050, Nov. 2016.

[8] K. A. Alobeidli, M. H. Syed, M. S. El Moursi and H. H. Zeineldin, "Novel Coordinated Voltage Control for Hybrid Micro-Grid With Islanding Capability," in *IEEE Transactions on Smart Grid*, vol. 6, no. 3, pp. 1116-1127, May 2015.

[9] M. M. Shabestary; Y. Mohamed, "Advanced Voltage Support and Active Power Flow Control in Grid-Connected Converter under Unbalanced Conditions," in *IEEE Transactions on Power Electronics* , in proc. 2016.

[10] I. M. I. Arias, "Grid Codes Comparison", Master thesis, Department of Electric Power Engineering, Chalmers University of Technology, Göteborg, Sweden, 2006.

[11] M. Tsili and S. Papathanassiou, "A review of grid code technical requirements for wind farms," in *IET Renewable Power Generation*, vol. 3, no. 3, pp. 308-332, Sept. 2009.

[12] 'Nordic grid code' (Nordel, January 2007)

[13] 'Grid code–high and extra high voltage' (E.ON Netz GmbH, Bayreuth, Germany, April 2006)

[14] 'The grid code, issue 3, rev. 24' (National Grid Electricity Transmission plc, UK, October 2008)

[15] 'Grid code–version 3.0' (ESB National Grid, Ireland, September 2007)

[16] F. Ion, A. Hansen, P. Soerensen, N. Cutululis, "Mapping of grid faults and grid codes", Technical report of the research project 'Grid fault and design basis for wind turbine', Risoe National Laboratory, Denmark, 2007.

[17] S. Mortazavian, M. M. Shabestary and Y. A. R. I. Mohamed, "Analysis and Dynamic Performance Improvement of Grid-Connected Voltage–Source Converters Under Unbalanced Network Conditions," in *IEEE Transactions on Power Electronics*, vol. 32, no. 10, pp. 8134-8149, Oct. 2017.

[18] K. Ma, M. Liserre and F. Blaabjerg, "Operating and Loading Conditions of a Three-Level Neutral-Point-Clamped Wind Power Converter Under Various Grid Faults," in *IEEE Transactions on Industry Applications*, vol. 50, no. 1, pp. 520-530, Jan.-Feb. 2014.

[19] X. Liang and J. Hofman, "Trip Curves and Ride-Through Evaluation for Power Electronic Devices in Power System Dynamic Studies," in *IEEE Transactions on Industry Applications*, vol. 52, no. 2, pp. 1290-1296, March-April 2016.

[20] M. Shabestary, M. (2015). A Comparative Analytical Study on Low-Voltage Ride-Through Reference-Current-Generation (LVRT-RCG) Strategies in Converter-Interfaced DER Units (Master's thesis), University of Alberta.

[21] M. M. Shabestary and Y. A. R. I. Mohamed, "An Analytical Method to Obtain Maximum Allowable Grid Support by Using Grid-Connected Converters," in *IEEE Transactions on Sustainable Energy*, vol. 7, no. 4, pp. 1558-1571, Oct. 2016.

[22] K. Kawabe and K. Tanaka, "Impact of Dynamic Behavior of Photovoltaic Power Generation Systems on Short-Term Voltage Stability," in *IEEE Transactions on Power Systems*, vol. 30, no. 6, pp. 3416-3424, Nov. 2015.

[23] J. Chen, L. Jiang, W. Yao and Q. H. Wu, "Perturbation Estimation Based Nonlinear Adaptive Control of a Full-Rated Converter Wind Turbine for Fault Ride-Through Capability Enhancement," in *IEEE Transactions on Power Systems*, vol. 29, no. 6, pp. 2733-2743, Nov. 2014.

[24] M. M. Shabestary; Y. Mohamed, "Analytical Expressions for Multi-Objective Optimization of Converter-Based DG Operation during Unbalanced Grid Conditions," in *IEEE Transactions on Power Electronics* , vol.PP, no.99, pp.1-1.

[25] M. Ashabani and Y. A. R. I. Mohamed, "Integrating VSCs to Weak Grids by Nonlinear Power Damping Controller With Self-Synchronization Capability," in *IEEE Transactions on Power Systems*, vol. 29, no. 2, pp. 805-814, March 2014.

[26] K. Sharifabadi, L. Harnefors, H. Nee, S. Norrga, and R. Teodorescu, "Design, Control, and Application of Modular Multilevel Converters for HVDC Transmission Systems", John Wiley & Sons, Ltd., 2016.

[27] A. Camacho, M. Castilla, J. Miret, R. Guzman and A. Borrell, "Reactive Power Control for Distributed Generation Power Plants to Comply With Voltage Limits During Grid Faults," in *IEEE Transactions on Power Electronics*, vol. 29, no. 11, pp. 6224-6234, Nov. 2014.

[28] M. Castilla, et al. "Voltage support control strategies for static synchronous compensators under unbalanced voltage sags," IEEE Trans. Ind. Electron., vol. 61, no. 2, pp. 808–820, Feb. 2014.

[29] J. Miret, et al. "Control scheme with voltage support capability for distributed generation inverters under voltage sags," IEEE Trans. Power Electron., vol. 28, no. 11, pp. 5252–5262, Nov. 2013.